

Insulator Icing Flashover

M. Farzaneh

NSERC / Hydro-Quebec / UQAC Industrial Chair on Atmospheric Icing of Power Network Equipment (CIGELE) and Canada Research Chair on Atmospheric Icing Engineering of Power Networks (INGIVRE), <http://www.cigele.ca>

Abstract- Atmospheric ice accretion, combined with pollution, has been identified as a significant risk factor in the reliability of line and station insulators in cold climate regions. Flashovers occurring on ice- and snow-covered insulators result from combinations of a number of factors. Electric fields modify the structure of ice, the shape and direction of icicle development, the distribution of liquid water and the geometry of air gaps that break up the continuous ice surface. Electric field strength and voltage polarity as well as corona space charge and ionic wind have demonstrable influences on the flashover process. Insulator icing flashover is also affected by changes in air temperature and several other environmental and meteorological conditions including ice type and structure. The presence of surface pollution and the rejection of ions from solid to liquid layers during the freezing and melting process also play a central role in the icing flashover of insulators, which can occur at normal operating voltage under the most adverse conditions. This lecture presents an overview of these phenomena and describes the interactions that lead to the initiation and development of discharges on the ice surfaces covering the insulators, as well as their evolution to flashover. The lecture also includes the modeling of these phenomena, leading to successful prediction of withstand voltage as well as to insight into the most practical solutions for improved insulator design and mitigating icing flashovers.

I. INTRODUCTION

In many parts of the world a wide variety of man-made structures, including overhead power lines and outdoor substations are affected by atmosphere icing, sometimes leading to serious failures and damage with major socioeconomic consequences. The disruptive effects of atmospheric icing are mainly the results of excessive ice accretion combined with the effects of wind and dynamic phenomena such as galloping and jumping of conductors caused by sudden ice shedding [1, 2].

Flashover across insulators, which is the main purpose of this lecture, is another source of failure. The main functions of outdoor power network insulators are to mechanically support high voltage conductors and to separate them electrically from other conductors or from the ground. The mechanical strength requirements of insulators are determined by loading conditions and their electrical requirements by the permanent and transient electrical stresses which they should withstand with a low probability of failure or flashover. As concerns the mechanical design specifications, these are fully developed and covered in standards, providing good results in a wide range of climates. The electrical design of insulators under icing conditions, however, is more challenging. In fact, due to the variety and complexity of the parameters and phenomena

involved, there is no equivalent standard-based design process as compared to mechanical ones.

Electrical performance of insulators is largely affected by the exposure to adverse environmental and climatic conditions. In polluted environments, typically a pollution layer containing mineral matter, conductive dust, and water soluble salts, is formed on the surface of insulators [3-7]. In cold climate regions, in addition to the pollution layer formed during cold periods, ice and snow accretion on their surfaces constitutes another type of pollution, essentially non-conducting at low temperature and thus an aggravating factor similar to non-soluble deposit density at normal temperatures [8]. Moreover the structure of ice deposits is affected by applied voltage and its polarity as well as by partial discharges during ice accretion [2].

Due to the migration of contaminants to the ice surface during the freezing process of water droplets and the deposit of additional ions generated by electrical discharges, the surface of the ice accreted on insulators is generally highly conductive [2, 8-10]. This causes enhancement of leakage current, a positive feedback resulting in further ice melting and eventual formation of a substantial film thickness of highly conductive water on the surface of the accumulated ice [8-10]. Such conditions generally lead to the enhancement of partial discharges and the formation of local arcs across the air gaps which may lead to the occurrence of a flashover arc. Flashover is the result of the complete bypassing of the electrical insulation by a breakdown path which is sufficiently ionized to maintain an arc short-circuiting a phase conductor or a high-voltage bus.

Incidents involving single-phase faults related to flashover of insulators during winter periods have been reported from various countries which experience atmospheric icing [11-24]. According to these reports the number of incidents increases during precipitation icing and after ice or snow accretion followed by a rise in air temperature above 0°C, causing melting. Although problems related to winter conditions have been occasionally reported at high-voltage transmission levels up to 230 kV with widespread use of extra-high-voltage (EHV) equipment in cold climate regions, insulator winter flashovers have been recognized essentially at EHV level, more particularly on polluted station insulators during melting periods. Farzaneh and Kiernicki in 1995 [25] presented one of the early reviews on insulator flashover under ice and snow conditions reported from 11 countries around the globe. Two years later, a detailed review of the North America experience was consolidated by Chisholm [26]. In 2005, CIGRE [27] carried out a survey related to insulator failures under winter conditions from 35 utilities on 400- to 735-kV line and station insulators. Specialized conferences such as the International

Workshop on Atmospheric Icing of Structures (IWAIS) have also devoted sessions to this topic, since 1982. Panel sessions and presentations were also organized regularly by a number of other conferences on high voltage and insulation such as ISH (International Symposium on High voltage Engineering), ICHVE (International Conference on High Voltage and Application), IEEE Electrical Insulation Conference (IEC) and IEEE Conference on Electrical Insulation and Dielectric Phenomena (CEIDP). Considering the widespread use of EHV overhead networks in cold climate environments and the challenges of ultra-high-voltage (UHV) engineering, guidelines were recently proposed by IEEE toward the testing, design and selection of insulators subjected to icing [28-34].

After a survey of atmospheric icing, this paper presents an overview of the phenomena influencing the structure of ice accretion on insulators and involved in the initiation and development of electrical discharges leading sometimes to flashover arcs. The paper also discusses the modeling of arc development, leading to successful prediction of the critical flashover voltage as well as to most practical solutions for improved insulator design and mitigating icing flashovers.

II. PROCESS OF ATMOSPHERIC ICE ACCRETION

Insulator icing and flashover, and the phenomena involved, cannot meaningfully be described before introducing the process of atmospheric ice accretion and its meteorological aspects. Atmospheric icing is a generic term referring to various processes whereby water in various forms freezes and adheres to the surface on an exposed object [1, 35, 36]. In general, these icing processes belong to the following categories:

- 1) *Precipitation icing* occurring in several forms such as freezing rain and wet or dry snow, depending on the temperature and its variation near the ground and up to a few hundred meters above the ground.
- 2) *In-cloud icing* involving the instantaneous freezing of supercooled water droplets in a cloud or fog upon their impact with an exposed object. Depending on liquid water content (LWC), size and distribution of the water droplets, as well as air temperature and wind speed, soft or hard rime may occur.
- 3) *Hoar frost* resulting from the deposition of interlocking ice crystals on an exposed object when air at temperature below the freezing point is brought to saturation by cooling.

These icing processes result in various types of atmospheric ice accretion on overhead transmission line equipment including outdoor insulators. The various types of ice accretions and their properties are summarized in Table I.

Insulators can be exposed to any of the atmospheric ice types presented in Table I. The amount of ice or snow accumulation, combined with some other major parameters such as contamination level on insulator surface prior to icing, air temperature and its variation, as well as the length, number and position of air gaps, are determining factors influencing the process of discharge inception and its development to flashover arc.

TABLE I
TYPES AND PHYSICAL PROPERTIES OF ATMOSPHERIC ICE

Type of ice	Density (kg/m ³)	Appearance and properties	Adhesion / cohesion
Glaze ice	700-900	transparent, grown in a wet regime sometimes with inclusions of air bubbles and often with icicle formation	strong/strong
Hard rime	300-700	opaque to transparent, grown in a homogeneous structure with air bubble inclusions	strong/very strong
Soft rime	150-300	white, granular structure	medium/low to medium
Wet snow	100-850	white, grown in various structures and shapes and may have high liquid water content	medium/medium to strong
Dry snow	50-100	white, grown in various structures and shapes	low/low
Hoar frost	< 100	white, needle structure	low/low

For a light amount of ice, if the temperature is below freezing point the role of this thin ice layer is to stabilize the contamination layer on the insulator surface. However, if the temperature rises to values above the freezing point, the ice layer melts and the insulator surface is wetted. This also happens with light amounts of wet or sticky snow. In both light ice or snow conditions, the process of arc initiation and development is similar to that of contaminated insulators in clean fog conditions.

If the amount of ice or snow is moderate or heavy, this can lead to the bridging of insulator shed spacings with ice and icicles or with snow sleeves. In such cases, ice and snow are typically accreted as a crescent shape, extended across the full insulator diameter, on the side facing into the wind and to precipitation direction.

In addition to wetting of insulator surface by wet snow, soluble ions tend to migrate within snow or ice layers. In the case of contaminated insulators, part of the contaminant particles on the insulator surface can also migrate to the ice surface or inside the wet snow. In addition to surface deposits, contaminant ions in supercooled precipitation or fog droplets are rejected from the solid portion toward the liquid portion of the droplets during the solidification process involved in wet ice accretion. Moreover during wet snow or ice accretion on energized insulators, one or several air gaps are formed along the insulator strings. All these processes and phenomena modify the electric field distribution along the affected insulators, reduce the leakage distance to values as low as the dry arc distance, which result in decreasing the electrical performance of insulators under icing conditions particularly at air temperatures around 0°C.

Glaze ice with icicles, grown in a wet regime and generally occurring during freezing rain precipitations, is recognized as the most dangerous type of ice accretion because it is associated with the highest probability of flashover occurrence on ice-covered insulators [2, 37]. This type of ice is

recommended in IEEE Standard 1783TM [33] for laboratory testing for cold climate regions.

III. EFFECTS OF ELECTRIC FIELD ON ICE ACCRETION

A. Effect of electric field on conductor ice accretion

It could be expected that dc polarity plays an important role in the accretion of ice on conductors. Insects are preferentially deposited onto the positive pole conductor surfaces, and repelled from the negative pole, in outdoor corona tests. Growth of hoar frost tendrils up to 150 mm have also been noted on the positive pole outdoors.

The characteristics of ice and icicles formation on an exposed, energized metal surface have been the subject of several studies [38, 39] for dc and ac. Effects of electric field are illustrated by showing ice accretion on a rotating aluminum cylinder [39]. The 25-mm cylinder in Fig. 1 was exposed in an icing wind tunnel to supercooled water droplets with volume-mean diameter of 40 μm and an ice accretion rate of 2.1 $\text{g}/(\text{m}^2\text{s})$, at an air temperature of -10°C . The structure and morphology of ice accretion were influenced by voltage polarity and electric field strength at the surface of the test cylinder. Figure 1 shows that the non-energized case had hard rime ice accretion with small protuberances on its surface, in contrast with thin radial feathery branches especially for the ac and dc positive applied voltage.

When the electric field was increased from 5 to 18 kV/cm at the cylinder surface [39], the density of ice decreased sharply from about 0.85 g/cm^3 to about 0.31 g/cm^3 , 0.18 g/cm^3 and 0.15 g/cm^3 under ac, dc+ and dc-, respectively. For an electric field lower than 5 kV/cm, no density change was noted on the conductor ice accretion.

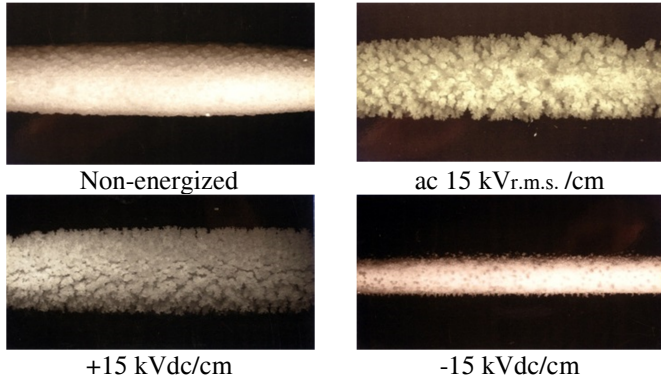


Fig.1 Effect of voltage polarity and electric field strength on ice accretion on a rotating 25-mm diameter aluminum cylinder [39]

B. Effect of electric field on insulator ice accretion

Voltage stress and polarity also affect ice accretion on the surface of insulators and on icicle formation around the sheds [40-42]. There are two significant changes that are noted when icing tests are carried out on insulators energized at normal line voltage. The first effect is a tendency towards radial outward displacement of long icicles as shown in Fig. 2 [42].

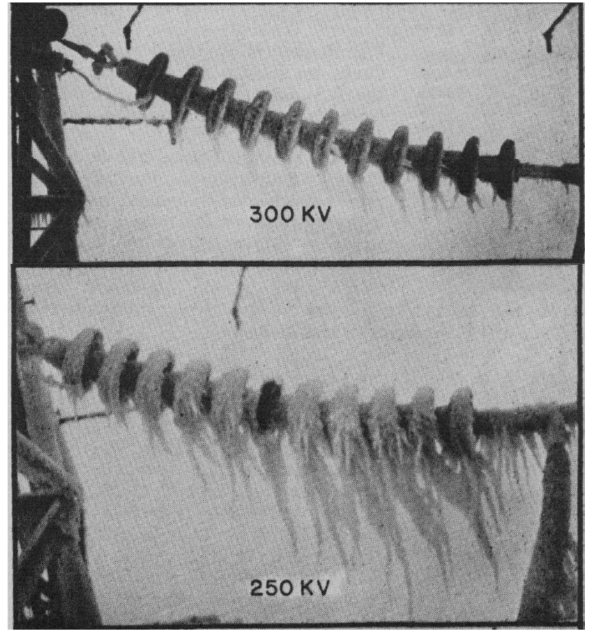


Fig.2. Effect of DC voltage on accretion of ice with applied water conductivity of $238 \mu\text{S}/\text{cm}$ on dead-end assembly [42]

Voltage polarity also affects the density and texture of wet-grown ice. Accretion of ice caps on the top surfaces of a vertical string of anti-fog porcelain disc insulators was investigated. The insulators were sprayed with supercooled droplets of 85- μm diameter at -10°C under non-energized and energized conditions of 15 kV_{r.m.s.} per disc under ac and 15 kV per disc under dc [40]. A typical line voltage stress would be 10 kV per 146 mm of cap-to-pin spacing, increasing to the test levels near the high voltage terminals. The intensity of ice accretion in this study was about 5.3 $\text{g}/\text{m}^2\text{s}$. The ice formed under these conditions was wet ice, as defined in Table 1, which promotes the formation of icicles. The density, air bubble features and grain texture of the ice were studied from thin sections prepared from bulk deposits on the top surface of the discs, as shown in Fig. 3.

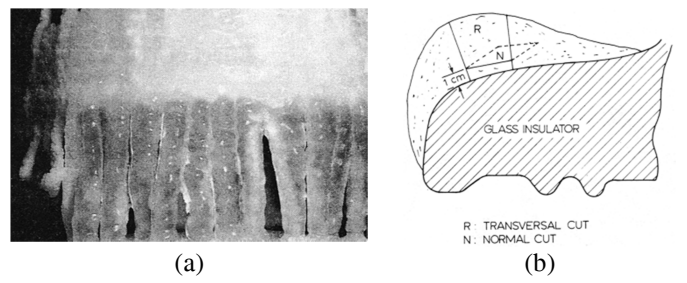


Fig.3. View of ice and icicle formation on an insulator disc (a) [41] and of the thin sections cuts used for density and microscopic study (b) [40]

The results obtained under the test growth conditions showed that the ice density measured was about 0.86 g/cm^3 for ac, dc- and dc+ applied voltages. This value was comparable, within experimental error, to the value of 0.87 obtained under non-energized conditions. It was also noted that the weight of the

ice and icicles accumulated during 1.5 h per disc was approximately the same (≈ 1.47 kg/disc) under ac, dc- and dc+ and about 10 % higher under non-energized conditions. This difference may be due to the heating effect of partial discharges and leakage current. No effect of voltage and polarity was observed in microscopic observation of air bubble features and grain texture. These findings were similar to those obtained for ice accretion on the rotating aluminum cylinder, suggesting that the mean field strength at the top surface of the insulator was also lower than 5 kV/cm during the ice accretion process.

The second effect of electric field, especially observed on EHV-class station post insulators, is the appearance of multiple air gaps, typically forming near metal hardware first. This effect is found for both dc and ac as shown in Fig. 4 [43]. In contrast to the findings for ice caps, electric fields exert a strong influence on icicle morphology and microstructure. Individual icicles grown under non-energized and energized conditions [41], under ac and dc were removed from the bottom of the insulators (see Fig. 3a). Then, thin ice films were cut at three cross-sections of individual icicles: top, middle and bottom [41]. Figure 5 shows photographs of the icicles and thin-section microstructures observed under ordinary and polarized light allowing bubble and crystal feature observation respectively [41].

This study confirmed that the icicles elongated as a hollow tube of ice with liquid water inside the tip as predicted by Makkonen's model [44] under non-energized conditions. As observed on thin cross sections (Fig. 5), microcavities at the center of the core and crystal features are both typical of water trapped in the hollow tube inside the icicle. It is possible that this water column inside of the icicle plays a role in arc development and decrease of insulator flashover voltage. However, this still needs to be further investigated.

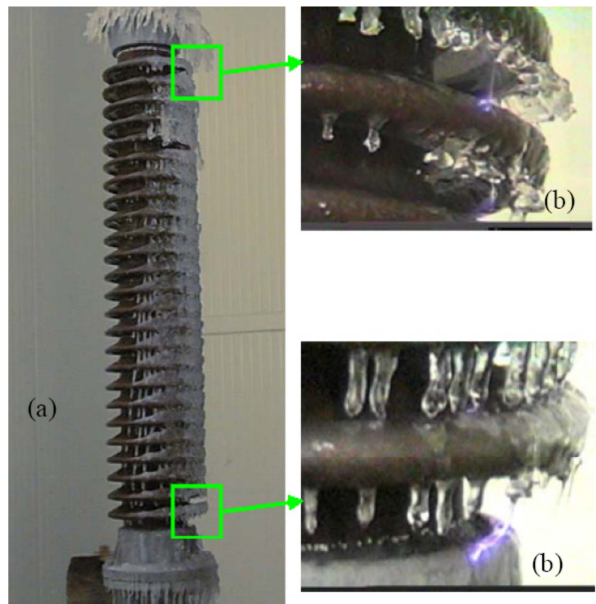


Fig.4. Icicles on an energized station post insulator: (a) ice-covered insulator with air gaps; (b) inception of corona discharges in ice-free zones [43]

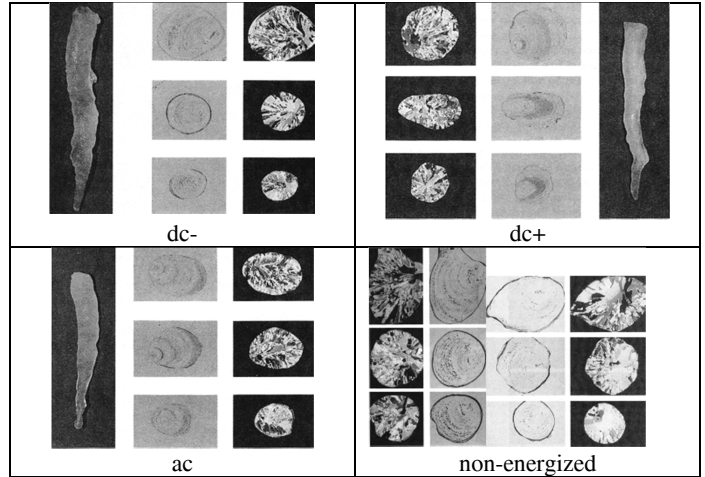


Fig.5. Icicle grown sample under energized and non-energized conditions with bubble feature and grain texture as observed in top, middle and bottom sections of icicles [41].

Under three energized conditions (dc-, dc+ and ac), the icicles were bent and slightly inclined toward the vertical axis of the insulator string. Also, from the thin film cross-sections of icicles, it is clear that voltage polarity has an influence on the elongation and reduction of the diameter of pendant water drops near the icicle tips.

The effects of electric field and voltage polarity on icicle growth down from the insulator skirts are clearly visible in Fig. 5. The dc- condition led to bubble and grain textures that were rather similar to the non-energized condition. A more pronounced effect was observed for ac and dc+, where the ionic wind velocity was found to be higher than under dc- [45]. Icicle growth is in fact very sensitive to heat balance conditions prevailing at water/ice interface, including sublimation of ice to vapor with an attendant heat of fusion loss of 334 Joules per gram. Ionic wind causes an additional and significant cooling effect which contributes to increased heat loss mainly at the icicle tip. More analysis of the effects of electric field and voltage polarity on the ice and icicle built-up on insulators under energized and non-energized conditions can be found in [40, 41].

IV. FLASHOVER PROCESS ON OUTDOOR INSULATORS

The flashover process on the ice-coated insulator has several different influences from environmental and meteorological conditions, notably temperature, icing rate and the electrical conductivity of the applied water as well as any pre-existing surface pollution [2, 8]. The applied electric field stress and polarity, partial discharge activity, leakage current along ice and icicle surfaces, water droplet elongation and ionic wind are other parameters influencing the flashover process [2].

Figure 6 shows the process of arc initiation and propagation along an insulator string covered with heavy wet-grown ice.

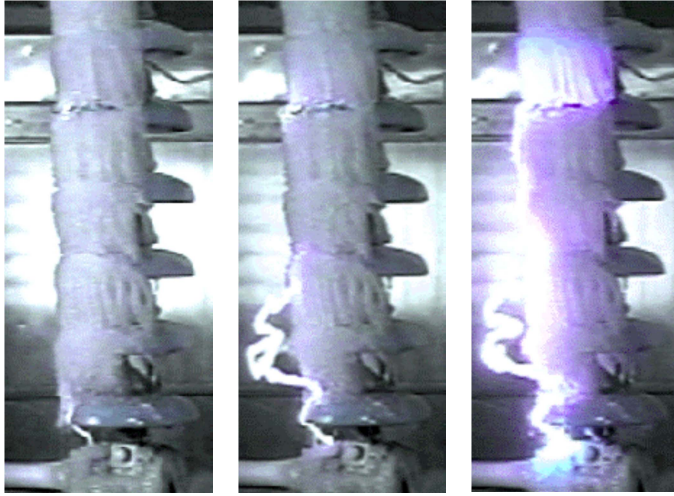


Fig.6. Process of arc formation and propagation [8]

A highly conductive layer on the ice is formed by rejection of ions to the surface water film from the water applied during accumulation. Heat inputs from leakage current and discharge activities, rising with air temperature or solar flux, can maintain the water film highly conductive without significant drip loss of ions during a slow melting phase. With the presence of this high-conductivity surface, most of the voltage applied to the insulator appears across the air gaps. In the case where the applied voltage is lower than the critical flashover of the insulator string, arcing activities cannot develop to flashover arc. However, for higher applied voltages, the violet arc appearing across the air gaps can transform to a white arc and propagate along the ice surface, resulting in a complete flashover arc. A flashover arc usually occurs when the length of the white arc reaches two-third of the insulator's dry arc distance, as shown in Fig. 6.

A. Discharge inception and propagation on ice surface

The flashover process in Fig. 6 starts with the initiation of partial discharges. In particular, streamer onset and propagation were studied on an ice surface between a rod-plane configuration half-submerged in ice bulk under lightning impulse voltage using streak photography techniques, as shown in Fig. 7. These studies also include corona discharge on an insulator surface and across the air gaps between electrodes [46-50]. These fundamental investigations, which are of general interest for the design of insulators subjected to icing, made it possible to better understand the discharge inception on the ice surface and to determine how the ice interacts with propagating discharge. They also allowed identifying a number of parameters including type of ice and its surface characteristics (uniformity and conductivity), surrounding air temperature, arcing distance, voltage characteristics (shape and polarity), electrode shape and its axis orientation which influence the discharge inception and propagation on the ice surface.

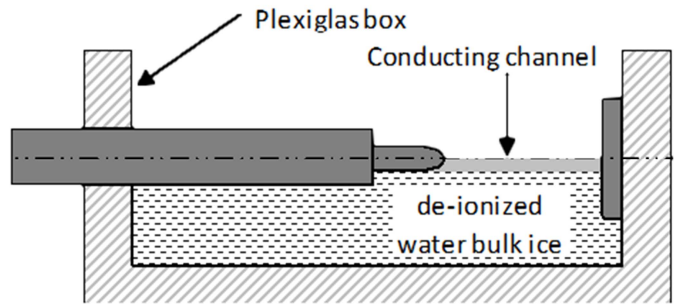


Fig. 7. Vertical cut of the ice model at test [49].

A streamer on the ice surface can be initiated by a free electron when an electric field above a certain critical value is applied to electrodes having a sufficient inter-electrode distance. Based on experimental investigations [48, 49], using the rod-plane configuration (Fig 7), the following empirical equation was derived to predict the streamer inception field E_{inc} (in kV/cm) on the ice surface as the function of freezing water conductivity σ (in $\mu\text{S}/\text{cm}$)

$$E_{inc} = A \cdot e^{-B\sigma} = (\alpha \cdot \ln(r) + \beta) \cdot e^{-B\sigma} \quad (1)$$

where A (in kV/cm) and B (in $\text{cm}/\mu\text{S}$) are constants and depend on the HV electrode radii r (cm) and the inter-electrode distance d as shown in Table II.

TABLE II
PARAMETERS A AND B AS A FUNCTION OF THE GAP GEOMETRY

Experimental conditions	Parameters defined in Eq. (1)
$d = 35 \text{ mm}$	$A = -49 \ln(r) + 45$ $B = 8.3 \times 10^{-4} \text{ cm}/\mu\text{S}$
$d = 70 \text{ mm}$	$A = -73 \ln(r) + 55$ $B = 8.3 \times 10^{-4} \text{ cm}/\mu\text{S}$

This empirical equations need to be generalized for a large range of d and σ values in future investigations.

Once the initial avalanche is produced, the streamer propagation may initiate the development of a new avalanche further along the ice surface. One of the possible mechanisms involved in streamer propagation on an ice surface is the release of electrons from the ice surface due to various mechanisms [49, 51], including photo-ionization close to the head of the discharge channel of the initial avalanche. Depending on the local electric field strength, multiple new avalanches can take place in a similar way until the discharge channel reaches the cathode and a breakdown of the ice surface has occurred. If the electric field is weak, the streamer propagation ceases and the space charge is diffused and absorbed.

A phenomenological sketch giving a better idea of the streamer propagation on an ice surface is presented in Fig. 8 [46].

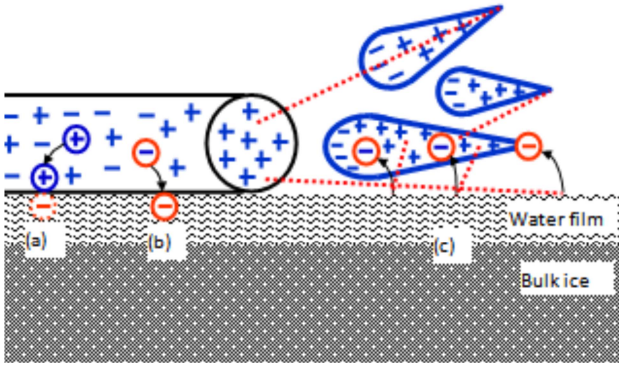


Fig. 8. Basic processes contributing to ionization and attachment in a streamer propagating on an ice surface: (a) positive ion capture by electrostatic forces; (b) electron capture in surface traps; (c) photoelectron extraction contributing to collisional ionization [46]

The ice surface properties are greatly governed by the liquid-like “water film” layer shown in Fig. 8. This layer persists for temperatures as low as -28°C and is also sensitive to salt dopants [52-54]. Due to the high conductivity of the liquid layer caused by rejection of impurities at the ice surface during the solidification process and the higher mobility of molecules in liquid, the streamer development becomes much faster. A simplified mathematical model for simulation of streamers dynamic behavior on an ice surface can be found in a previous study [51].

Melting tends to reduce the interfacial free energy, increasing surface conductivity. This is also supported by the observation that the mechanical disturbance of an ice surface increases the surface conduction since it produces many lattice defects and electrically-mobile ion states in the surface region. Avalanche growth and streamer propagation on an ice surface could, therefore, be controlled by increasing the ionization coefficient because molecules in such a layer are more mobile and electrically active defects are more abundant. Increased ice surface conductivity could also lead to a much faster streamer development. The process of ionization involves the dissociation of molecules or ionic crystals into ions when the surface melts. It is to be emphasized that photoionization in air results only from photons of energy higher than the following ionization threshold: $h\nu \geq 12.08\text{ eV}$ for oxygen molecules and $h\nu \geq 15.58\text{ eV}$ for nitrogen molecules. Comparing the energy for the photo-ionization with the work function of NaCl and derivate atoms, it is found that the former value is about 1.5 to 3 times larger than the latter. Since the surface discharge develops close to the ice surface; therefore, the sources of photons must also be very close to the surface. This suggests that in the case of ice surface discharge development, the produced photons irradiate the ice surface which in turn emits electrons.

B. Characteristics of arc propagation over an ice surface

Using an ultra-high speed image recording technique, several parameters of an arc propagating over an ice surface such as channel radius, foot shape and propagating patterns were studied recently [55]. Figure 9 shows a simplified ice

geometry consisting of a 140 cm (L) x 15 cm (W) x 5 cm (D) Plexiglas mold with ice. The ice was made of de-ionized water. A narrow band of about 5 cm width and 3 cm depth was made along the ice surface and filled with water of predetermined conductivity before it was frozen in a cold room to obtain a conductive ice band. After the conductive band was formed, the HV electrode was positioned with a 6 cm air gap and the far end of the model was grounded using a flat metal surface [56].

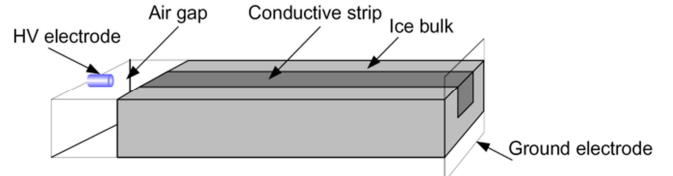


Fig. 9. Simplified geometry ice model [56]

The models were placed vertically in front of an ultra-high speed camera either in both propagating-upward and propagating-downward arc directions. Experimentally, the arc buoyancy exerts some influence on the arc constants relating voltage drop and current. An image intensifier was placed in front of the camera to observe the ultraviolet (UV) light at the tip of the propagating discharge on the ice surface. The air temperature was adjusted to stay above the freezing point to maintain a water film on the ice surface. The ac voltage was then increased till thin filamentary violet partial discharges appeared across the air gap. These discharges first appeared with a common bright root (stem) emitting high intensity UV light, decaying in length and intensity as leakage current passes through zero twice every cycle. Then, discharges reappeared along the air gap after each re-ignition, before continuing to propagate over the ice surface. At early stages, the discharge length increases slowly after each re-ignition with the discharge tip emitting more UV light compared to the discharge channel. This is probably due to the fact that the channel ionization is mostly governed by thermal ionization, emitting the light in the visible region, whereas the ionization at the tip of the discharge is collision ionization [55].

Leakage current during the propagation of discharge on the ice surface increases continuously. When it reaches a value of about 20 mA, the thin filamentary violet partial discharges suddenly transform into a bright white arc with a non-uniform diameter as illustrated in Fig.10 for a positive arc (dc+) for top (a) and bottom (b) air gap positions. The arc radius depends greatly on the leakage current but also on environmental conditions including temperature, humidity and pressure [2, 57]. The central core of the white arc is very bright compared to the surrounding envelope.

The high-speed UV camera observations showed that the arc does not propagate in complete contact with the ice surface and that only the arc foot is in contact with the ice surface. The shape of contact surface appears branched, each branch carrying part of the arc channel current to the ice surface (Fig. 10). The results also show that the arc is initiated across the air gap and propagates with a moving foot on the ice surface.

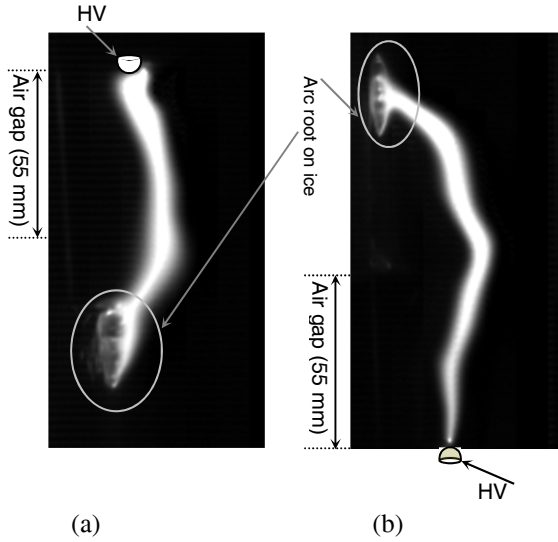


Fig.10. Arc channel corresponding to top (a) and bottom (b) air gap positions [56]

C. Arc propagation velocity on an ice surface

In a recent study, arc propagation was studied over an ice-covered insulator with a dry arc distance of 1.73 m. The arc propagation process is completed in three stages. The first stage starts from the moment the arc along the air gap starts to propagate slowly over the ice up to about 40% of the insulator dry arc distance. In the second stage, the arc continues to propagate up to 80% of the dry arc distance with a much higher velocity. The third stage corresponds to the final jump (flashover) at which arc velocity propagation reaches its maximum value. [58]

Table III shows the arc propagation velocity at different stages for various applied water conductivities (σ), under dc and ac, as measured by ultra-high speed photography technique [58]. It can be seen that, depending on the voltage type and freezing water conductivity, the maximum velocity varies in the range of 1000 to 2000 m/s.

Table III.

PROPAGATION VELOCITIES OF AC AND DC ARCS ON AN ICE-COVERED INSULATOR

voltage type	σ ($\mu\text{s}/\text{cm}$)	Arc velocity (m/s)		
		Stage 1	Stage 2	Stage 3
ac	80	0.58-2.96	218-272	984-1154
	150	0.54-3.12	415-446	1450-1857
dc+	80	0.45-2.74	215-242	867-1108
	150	0.47-2.84	413-461	1363-1533
dc-	80	0.52-2.87	204-232	1043-1384
	150	0.54-3.24	407-524	1674-2106

The increase of arc propagation velocity from one stage to the other as well as its increase as a function of σ is due to the increase in the energy supplied to the arc channel resulting from the increase in leakage current through the ice surface. Leakage current increase is due to increasing ice melting, resulting in higher arc propagation velocity. Leakage current also increases as applied water conductivity (σ) is raised, resulting in increased arc propagation velocity. Moreover, for a given applied water

conductivity, the dc- propagation velocity at the last stage is higher than that of dc+, with the ac velocity in between. This may explain why critical flashover of an ice-covered insulator is lower under dc- than under dc+ [58].

D. Arc evolution to flashover

AC flashover on ice-covered insulators has been widely studied, including establishing the necessary reignition coefficients for buoyant arcs (energized from a phase conductor below an insulator string) as well as arcs that must move down an energized post insulator from above. Additional refinements include the effect of multiple arc root voltage drops across air gaps [59], and the dynamic behavior of the arc itself. In contrast, the evolution of DC arcs to flashover on the distance scale greater than 1 m has not had similar experimental support until recently [58, 60-62]. In some ways, dc arc evolution to flashover is simpler than ac, because reignition does not occur, but the interaction of dc arc current with ice layer temperature, chemistry and resulting surface layer conductivity involve several branches of physics.

The typical model for dc flashover [8] uses a pair of fixed values A and n to relate arc voltage gradient (kV/cm) to current (I) with the form $V/x = A I^n$. Some arc constant values date back to Ayrton and Steinmetz. They have a wide range depending on surface chemistry and current. The arc coefficients also depend on whether the arc is stationary or moving along the ice surface [8, 63]. For the case of interest, the coefficients $A=204.7$ and $n = 0.66$ were fitted to arcs on ice surfaces as shown in Fig. 11.

Novak and Ellena [64] noted a transition from $n=0.81$ to $n=0.54$ for dc arc currents above and below 1 A, as well as a transition from glow discharge to arcing at 300 mA. Over this same current range, Nekahi and Farzaneh [65, 66] established with spectroscopy that the arc rotational temperature varied from 4000 to 6500 K as shown in Fig. 12, while the excitation temperature was relatively constant at 9000 K.

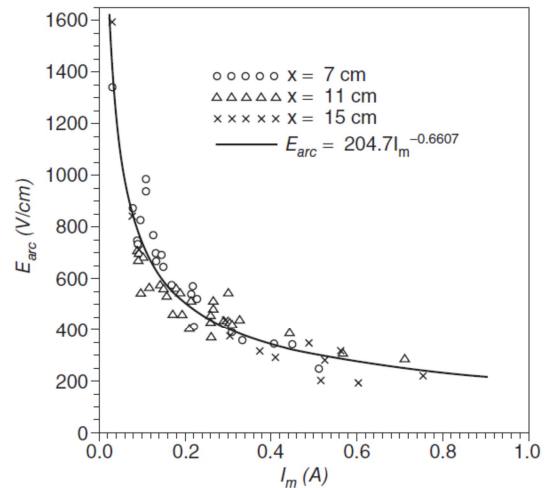


Fig.11. Voltage-Current Relation for Electric Arc on Ice Surface [67]

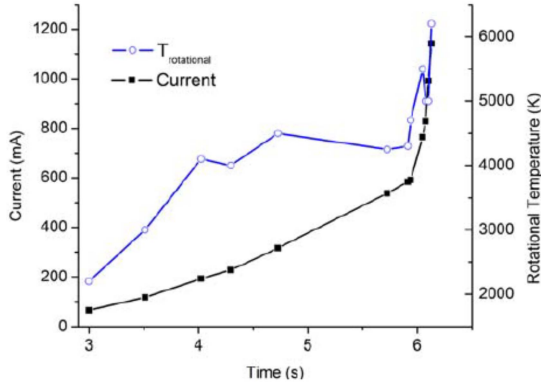


Fig.12. Evolution of DC arc current (left scale) and rotational temperature measured by spectroscopy (right scale) [65]

Fixed values of A and n may only be appropriate for the stage shown in Fig. 12 from 4 to 6 seconds, where the rotational temperature is constant at 4000 K. Additional links between measured arc temperature and values of A and n remain to be explored.

E. Prediction of Insulator Flashover Voltage

The simplest model for predicting flashover voltage of fully-iced insulators assumes that the product of the ice weight w (g per cm of dry arc distance) and the conductivity of the melted ice σ_{20} ($\mu\text{S}/\text{cm}$) defines the effective resistance of the ice layer [8]. The product $w \cdot \sigma_{20}$ is called the icing stress product (ISP). The critical flashover stress E_{50} , in $\text{kV}_{\text{rms}}/\text{m}_{\text{dry arc}}$, is given by:

$$E_{50 \text{ ac}} = 396(\text{ISP})^{-0.19} \quad (2)$$

This expression is valid for ice accretion under normal line voltage and ac flashover during a melting phase. For tests using multiple -dc flashovers on an ice layer formed without line voltage stress, the critical flashover stress has been found by Jiang et al. [60] to be:

$$E_{50 \text{ dc-}} = 1174(\text{ISP})^{-0.26} \quad (3)$$

The expressions (2) and (3) describe many experimental results in the practical range of $10^3 < \text{ISP} < 10^5$.

Linearity of flashover stress along the dry arc distance, in the range of 0.5 to 4 m, has been established for ac. Recently, Li et al. [68] established a modest degree of nonlinearity for dc flashover of iced insulator strings, with $E_{50} = 125 \text{ kV/m}$ for 1.6-m strings declining to 90 kV/m for 5.5-m strings under the same icing conditions.

The Obenous model of an arc in series with a distributed resistive layer has been successful for basic modeling of the icing flashover process [67]. The flashover model sums the voltage drop along the arc and the voltage drop from current flow in the residual ice layer as follows.

$$V_m = A \cdot x \cdot I_m^{-n} + I_m R(x) \quad (3)$$

Where V_m is the peak value of the applied voltage (V), x is the total arc length (cm), $R(x)$ is the residual resistance of the

ice layer in Equation (4) and A and n are the arc constants as derived in Fig. 11. The resistance $R(x)$ is [67, 69]:

$$R(x) = \frac{1}{2\pi\gamma_e} \left[\frac{4(L-x)}{D+2t} + \ln \left(\frac{D+2t}{4r} \right) \right] \quad (4)$$

Where L is the length along the dry arc distance (cm) of the half - cylinder of ice, D is the diameter (cm) of the insulator, and γ_e is the equivalent surface conductivity of the ice layer (μS). The parameter t is the thickness of the ice layer and r is the effective arc root radius, considering the multi-point terminations seen in Fig. 10.

The effective arc root radius r in (4) is normally taken as a constant times the square root of current, with values of $r = 0.7 \sqrt{I}$ valid for dc arc currents I (A) and $r = 0.6 \sqrt{I_{pk}}$ for the peak ac current (A).

The equivalent surface conductivity γ_e (μS) is linearly related to the applied water conductivity σ_{20} ($\mu\text{S}/\text{cm}$) in a well-defined geometry. This relation can be applied to calculation of the resistance per unit length of a half-cylinder of ice that forms around a typical insulator, using for example $\gamma_e = 0.0675 \sigma_{20} + 2.45$ [67] for ac, other values (Table IV) for dc [2] or a simpler form $\gamma_e = k \sigma_{20}$ implied in the icing stress product (ISP) formulation.

Table IV.
RELATIONS BETWEEN SURFACE CONDUCTIVITY AND APPLIED WATER CONDUCTIVITY

ac	$\gamma_e = 0.0675 \sigma_{20} + 2.45$
dc+	$\gamma_e = 0.0820 \sigma_{20} + 1.8$
dc-	$\gamma_e = 0.0599 \sigma_{20} + 2.6$

If the applied voltage is sufficiently high and the critical conditions are reached, the local arc will develop to a flashover arc for dc conditions. As identified by Rizk [57], an additional reignition condition must also be satisfied: the voltage on a subsequent ac cycle must be sufficiently high to re-illuminate the arc channel after it is extinguished at every current zero crossing. High-speed cameras show the progress and retreat of the ac arc on every half cycle of applied voltage as shown in Fig. 13 [8].

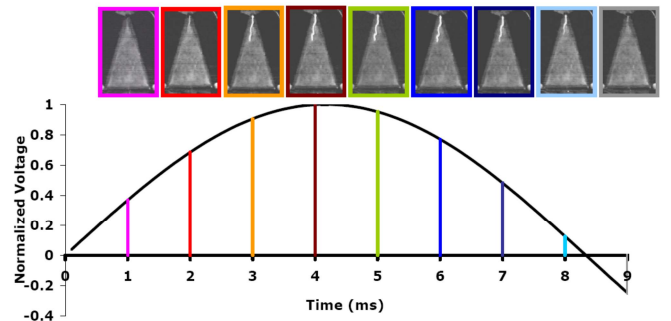


Fig.13. Variation of arc length on 250-mm tall by 200-mm wide ice sample under 60-Hz ac voltage. Frame rate of 1 ms [8]

For flashover across the dry arc distance, the reignition condition becomes:

$$V_m \geq \frac{kx}{l_m^b} \quad (5)$$

Reignition coefficients depend on whether the arc is buoyant (energized from below) with $k = 1118$, or descending vertically with $k = 1300$, and exponent $b=0.53$ in both cases. Recently, the ac reignition characteristics of an ice-coated externally gapped metal oxide resistor [70] were established to follow the same reignition equation as ice-coated insulating surfaces.

The simple arc model in series with a resistive pollution layer can be extended to include the series inductance of the arc as well as the capacitance from arc tip through free space to the ground electrode [71, 72]. The extra capacitance contribution of the ice layer, with its high relative permittivity, is ignored because its cross section is small. The circuit terms combine to form a dynamic model with improved time-domain response of the leakage current waveform. The L di/dt voltage drop appears in series with the AxI_m^{-n} term in Equation (3). The current flow I_m is increased by the C dV/dt term through free space. The arc inductance and capacitance both increase as the arc propagates down the ice layer, with increasing arc length x and decreasing ice layer length $L-x$. Using some approximations [73], the circuit values are:

$$L_{arc} \approx \frac{\mu_0}{2\pi} \left[0.25 + \ln \left(\frac{100 m}{r} \right) \right] \quad (6)$$

$$C(x, t) = 2\pi\epsilon_0\alpha \left[1 + \frac{r}{L-x} \right] \quad (7)$$

Where $\alpha = 1 - 1/\sqrt{1 + \left[\left(\frac{\phi}{2L} \right) \left(\frac{1}{1-x/L} \right) \right]^2}$, ϕ is the ground electrode diameter and r is the arc root radius.

Recently, this dynamic model for the ice flashover arc was extended to the case where there are two arcs in series with a floating ice layer [74]. The inductance terms for each arc were included and the model was simplified by ignoring the effects of capacitance. The effective series arc inductance doubles, and the series resistance includes the effects of current concentration at two arc roots, rather than one when there is a single ice layer as in Fig. 14.

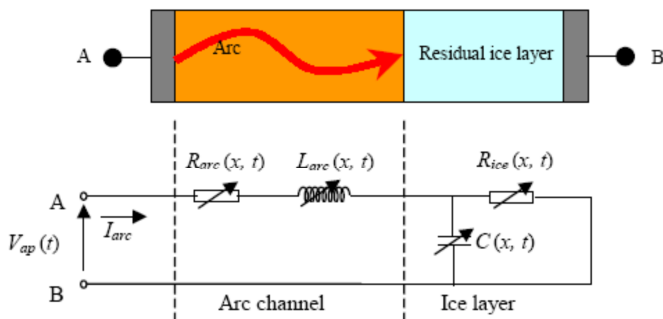


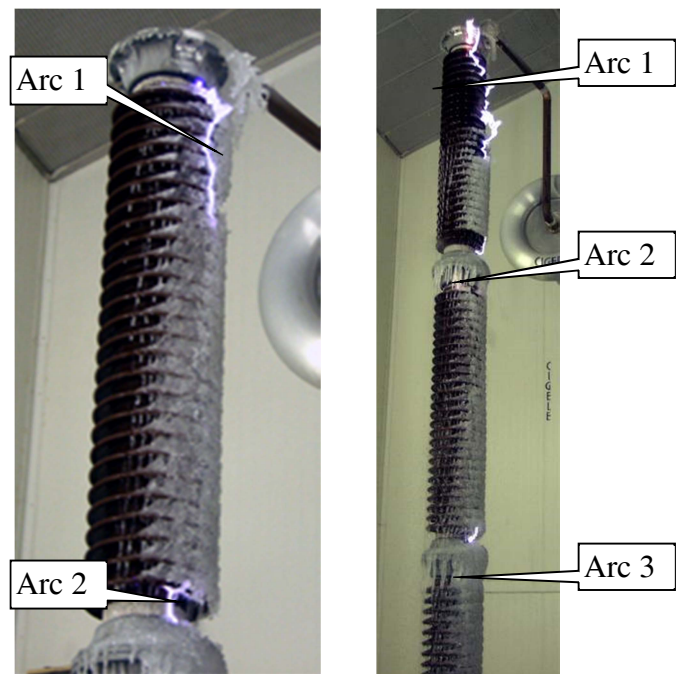
Fig.14. Dynamic model of ice layer flashover [70]

Figure 15 illustrates the formation of two arcs on a station post insulator with 1.4 m dry arc distance, and a third arc on an EHV post with 3.5 m. In the first case, there are two arc

roots on the ice surface and two on the metal end fittings. In the second case, there are a total of four arc roots on ice layers. To generalize, there are N' arcs from the metal electrode to the arc surface, and N'' arcs across the air gaps from ice surface to ice surface. The total number of arc roots N is then the sum of N' and N'' . Since the anode and cathode voltages for arcs on metal electrodes can be ignored, especially for ac conditions, only the voltage drops associated with the arc roots on ice surfaces need to be modeled. [59]. This is achieved with the use of the effective arc foot radius and the revised equation for $R(x)$ (Ω):

$$R(x) = \frac{10^6}{2\pi\gamma_c} \left[\frac{4(L-x)}{D+2t} + (N' + 2N'') \ln \left(\frac{D+2t}{4r} \right) \right] \quad (8)$$

Where γ_c (μS), L (cm), x (cm), and r (cm) have been defined previously, D (cm) is the insulator diameter and t (cm) is the ice thickness.



1.4 m dry arc distance 3.5 m dry arc distance
N=2 N=4

Fig.15. Typical Arcs and Air Gaps on Station Post Insulators in Icing Conditions [59]

V. SELECTION PROCESS FOR OUTDOOR INSULATORS IN FREEZING CONDITIONS

Icing flashover problems are statistically rare events and can be treated with some of the same approaches used for lightning protection. There will always be some towers with poor grounding that may be struck by a high-amplitude flash, leading to impulse backflashover. There will always be some towers that will have a combination of ESDD, ice weight w and applied water conductivity σ_{20} that combine to a high

value of ISP , leading to line-voltage flashover in melting conditions. Adaptation of log-normal distributions for icing parameters is one innovation, borrowed from lightning protection practice, which is found in IEEE Standard Project P1820 [34]. Lightning protection practice also establishes some reasonable expectations for reliability design under icing conditions, such as the one-in-200 year flashover failure rate at substations and less than 1 flashover per 100 km of line length per year for transmission lines having Class-B security.

A. Statistical properties of natural ice and pollution

Dedicated studies dating back to the 1960s have shown that precipitation conductivity, averaged among tens of observation sites over a year, tends to have site-specific log-normal distributions. With a log transformation, skew and kurtosis then approximate normal distributions. The standard deviation of a log-normal distribution is dimensionless, and typical values of 0.75 are found for natural logarithm of precipitation conductivity.

There are relatively few measurements of ESDD from outdoor monitoring sites. A review of seven sets of results, in Sweden and South Africa [75], suggests they share a common value of natural log standard deviation of 0.5, with median ESDD that varied from 0.0005 to 0.17 mg/cm².

Field observations have established that up to 90% of the road salt pollution found in natural ice accretion on insulators was from the surface ESDD, with the natural conductivity of the rain providing only 10% of the total ion concentration. The combined effects of pre-existing surface pollution and applied water conductivity have been evaluated theoretically and experimentally [60]. There remain some questions about the limited contribution of *ESDD* to the ice layer σ_{20} from any insulator surfaces that are not coated with ice.

There are few long-term measurements of ice accretion weight or thickness. The 59-year sample of data from Czech Republic reported in [76] has a standard deviation of natural log of ice weight of 0.83.

For comparison purposes, the standard deviation of natural log of peak negative lightning return stroke current is 0.61. The corresponding range of values for natural log of soil resistivity and unmodified footing resistance from tower to tower along a line is 0.9 to 1.0. Unlike the icing problem, where increases in ice weight w tend to dilute *ESDD* and reduce σ_{20} , the peak current and the footing resistance are independent variables.

B. Testing Facilities and Methods

A wide variety of test methods have narrowed down to acceptance of IEEE Standard 1783TM [33] for most practical purposes. This standard draws from pre-existing practice [77] for the selection of applied water conductivity ($\sigma_{20}=100 \mu\text{S}/\text{cm}$), specific *ESDD* levels and adequate power supply regulation for satisfactory reproducibility among laboratories. Continuous current draw in heavy icing tests typically exceeds that found in standard clean-fog tests, and this can be a challenge especially for dc tests.

Flashover level declines with increasing temperature below freezing. This is exploited both in the cold-fog test process in

IEEE 1783TM [33], where the surface can be re-iced with fog and retested, and in a U-curve testing approach used at Chongqing University [78]. A comparison of the U-curve approach and other methods to establish U_{50} [78] suggests that the results are closely linked by a relative standard deviation of about 5.4% for all test methods.

C. Application guidance for dry arc distance

The choice of insulators for icing conditions may prove to be the limiting constraint on dry arc distance and dimensions for UHV lines. The flashover stress is relatively constant in the range of $E_{50}=70 \text{kV}/\text{m}_{\text{dry arc}}$ for well-executed heavy icing tests that include an energized accretion phase and a melting phase [8, 33]. To a large extent, this explains why icing flashovers tend to be EHV/UHV problems. Typical 14-unit strings on 230-kV lines have a normal line voltage stress of about 65 kV/m of dry arc distance and it was only with the successful control of switching surge overvoltages at terminal equipment in the 1960s that higher stress levels were adopted for 345-kV, 500-kV, 735-kV and now 1000-kV lines.

Selection of insulators must consider the ice accretion level, as in Table V, which has a strong influence on the ranking of mitigation measures.

Table V.
CLASSIFICATION OF ICE ACCRETION SEVERITY BASED ON ENERGIZED PORCELAIN
INSULATORS [8]

Ice Accretion Level	Ground-Level Ice Thickness	t , reference ice level on rotating cylinder	Deposit on uniform profile station post	Deposit on 146x254 mm ceramic disk string
Very Light	< 2 mm	< 1 mm	No icicles; thin ice layer on all surfaces	
Light	< 12 mm	< 6 mm	Partially bridged with icicles	
Moderate	12-20 mm	6-10 mm	Fully bridged with icicles	Partially bridged with icicles
Heavy	> 20 mm	> 10 mm	Fully bridged with icicles	

There is general agreement that E_{50} under these conditions has a power-law relation:

$$E_{50} = K \cdot w^{-\alpha_1} \cdot \sigma_{20}^{-\alpha_2} \cdot ESDD^{-\alpha_3} \quad (9)$$

Where K is an empirical constant, w is ice weight per cm of dry arc distance, σ_{20} is applied water conductivity corrected to 20°C and *ESDD* is the surface pollution level, expressed as mg of NaCl per cm².

Each insulator has a unique relation between w and t , the thickness of ice accretion on a reference cylinder shown in Table V. Analysis of the ice weight on insulator profiles in IEEE P1820/D7 uses a simple estimate that w (g/cm dry arc) = $0.015 \cdot \phi \cdot t$ where ϕ is the diameter of the largest shed (mm), and t is the ice accretion thickness on a rotating reference cylinder.

In heavy icing tests, the three exponents in (9) tend to converge to $\alpha_1 = \alpha_2 = \alpha_3 = 0.19$ for ac (2) and perhaps to 0.26 for negative dc (3).

D. Application guidance for leakage distance

For very light icing, additional ice accretion merely dilutes the pre-existing surface pollution, which typically has a

conductance well in excess of usual values of σ_{20} . Flashover stress thus becomes a function of insulator leakage distance. The exponents α_1 and α_2 for cold-fog conditions with $t < 1$ mm fall to zero, and α_3 tends towards 0.36. This is the same exponent found in clean-fog tests [79].

The role of insulator leakage distance depends to a large extent on the degree of ice bridging. This was well illustrated by tests on twelve different profiles of nonceramic insulators [80] with a range of creepage factor C_f , the ratio of leakage to dry arc distance, of $2.8 < C_f < 4.0$. Figure 16 shows that, for 5 mm of ice accretion, peak performance is given by profiles with a creepage factor of 3.3. However, with increasing levels of ice accretion, the effect of C_f becomes unimportant as the relevant electrical distance becomes the dry arc distance alone.

When the IEEE P1820/D7 estimate of ice weight, $w = 0.015 \cdot \phi \cdot t$, is used to calculate the ISP for the twelve profiles tested in [80], along with $\sigma_{20} = 120 \mu\text{S}/\text{cm}$, the predicted critical flashover stress is in good agreement with the test results for very heavy accretion as shown in Fig. 17.

The relatively good agreement for severe 30-mm ice levels in Fig. 17 is also an encouraging point of common international agreement, especially considering that the experimental results in [80] were obtained using an icing period without normal line voltage.

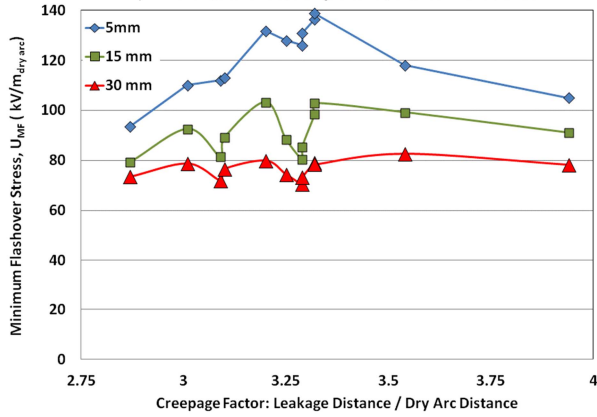


Fig.16. Effect of creepage factor on minimum flashover stress for twelve profiles of nonceramic insulators [data from 80]

VI. IMPROVED INSULATOR ICING FLASHOVER PERFORMANCE

Many mitigation options for improving performance of ice-coated insulators were set out and ranked in [8, 28-32]. Since that time, additional testing and field experience has been gained, and new technologies have evolved.

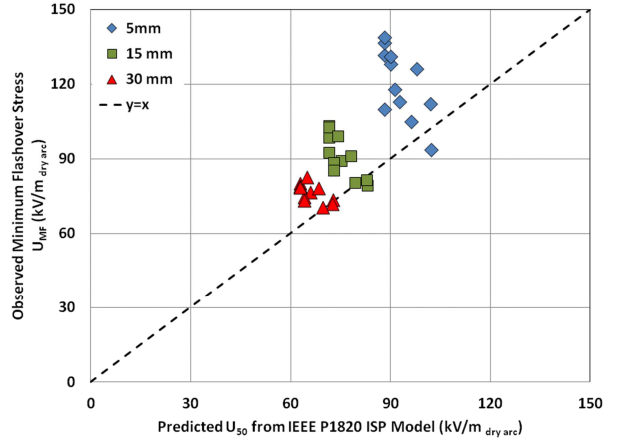


Fig.17. Relation between predicted ac critical flashover stress with ISP model and experimental data on twelve NCI profiles [80]

A. Corona Rings

It is somewhat counter-intuitive that the application of corona rings can degrade rather than improve flashover performance in icing conditions. The uniform electric field of an effective corona ring on the insulator surface tends to promote full ice bridging rather than formation of air gaps near the high voltage terminal as shown in Fig. 18.

Electrical performance of an EHV station post insulator was improved, rather than degraded, when the upper surfaces of corona rings were covered with a fine metallic mesh [81]. This prevented ice accumulation as shown in Fig. 19, leading to the improved flashover strength predicted by the multi-arc model, Equation (8) and [59].

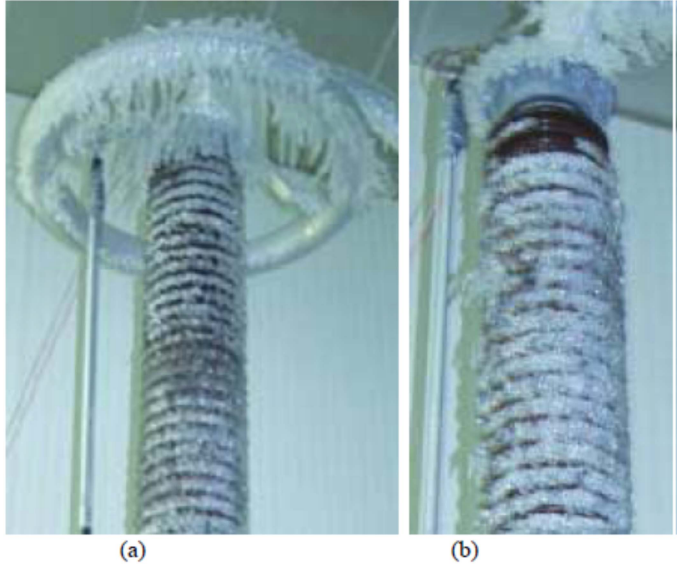


Fig.18. Ice accumulation on station post insulator, with (a) and without (b) grading ring [81]



Fig.19. Ice accumulation on station post insulator, with modified, screen-covered grading rings [81].

Icing tests on 230-kV class transmission line surge arresters demonstrated a second problem with corona rings in icing conditions with $t = 20$ mm, $w = 75$ g/cm and $\sigma_{20} = 30 \mu\text{S}/\text{cm}$. The ice accumulation at the energized, upper end of the arrester in Fig. 20 is similar in both cases. The low external flashover voltage for the double-ring treatment related to the fact that it reduced the dry arc distance compared to a single ring.

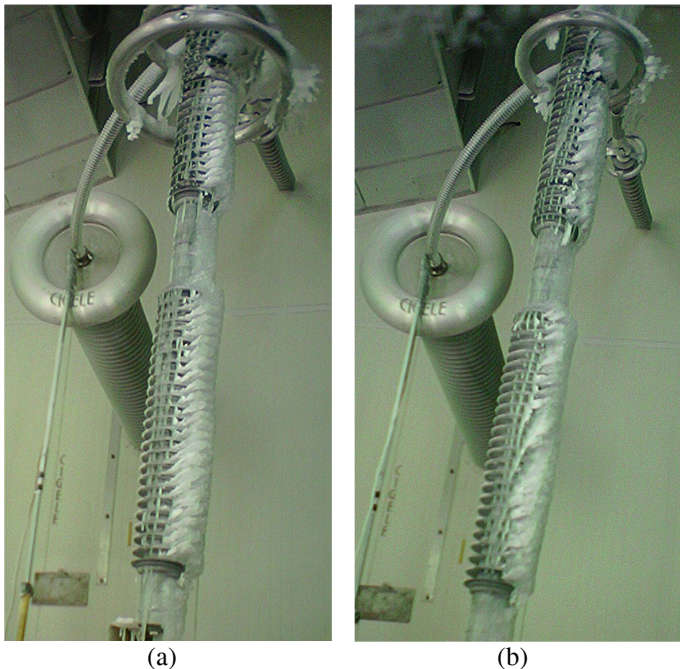


Fig.20. Ice accumulation on transmission line surge arrester with (a) double and (b) single corona ring [70]

Upper-section partial flashover is common in icing conditions and this represents a significant problem for surge arresters. Line voltage tends to overstress and fail the MOVs in lower units once an upper unit flashes over. This has caused an in-service failure of a 500-kV station arrester.

B. Insulator Coatings

RTV silicone coatings, applied to bushings and insulators have given good long-term performance in areas of road salt and industrial pollution, combined with very light or light icing. Recently, the coatings have been modified in two ways to mitigate heavy icing problems.

- Doping with carbon to make the coatings semiconducting, with sufficient current flow to prevent ice formation [82]
- Blending with materials that give sub-micrometer scale features that render the surfaces super-hydrophobic, self-cleaning and icephobic [83]

Problems with continuous current flow and power consumption through a semiconducting RTV coating can be addressed by introducing air gaps, for example coating only the bottoms of suspension disk units [82].

At present, stress-grading coatings that limit electric field to 10-15 kV/m have been evaluated for improved cable termination and winding performance, and if these exhibit sufficient durability in outdoor conditions they may also prove to be of interest for mitigating icing flashovers.

C. Booster Sheds

Booster sheds are accessories whose role in improving flashover performance in heavy rain conditions in excess of 5 mm/minute is understood [84]. Their application for icing conditions relies on the formation of additional air gaps [8, 85] in a wide range of conditions.

VII. CONCLUSIONS

Atmospheric ice accretion onto insulator surfaces presents a significant electrical flashover risk.

The electric fields affect the growth and morphology of icicles. These tend to grow radially outward in areas of higher electric field.

Detailed investigation of the ice flashover process shows that it generally follows the Obenous model of an arc in series with a distributed resistive layer. The arc constants and pollution layer resistance for icing conditions have been established. The effective radius of the arc root on an ice surface actually represents the net voltage drop of a multi-point contact. The arc floats above the ice surface in air except at this arc root.

Arc propagation velocity, rotational temperature and the arc constants themselves may have three separate phases: glow discharge below 200 mA, a period of extension at constant temperature of 4000 K, and a rapid current rise above 600 mA to flashover with rotational arc temperature of 6000 K.

For calculating the electrical performance of EHV insulators, the additional voltage drops of every arc root on the ice surface must be included, forming a multi-arc model.

The flashover stress, expressed in kV of line to ground voltage per meter of dry arc distance, has been found by several researchers to be a power-law function of the icing stress product (*ISP*), formed by the product of ice weight per cm of dry arc distance and the conductivity of the melted ice layer s_{20} , corrected to 20°C. Any pre-existing electrically conductive surface pollution, expressed as *ESDD*, increases σ_{20} and the *ISP*. Flashover stress for both ac and negative dc conditions follows the model over two orders of magnitude of *ISP*.

The efforts to standardize on icing test methods, leading to IEEE Standard 1783/2009™ [33], are mostly complete worldwide. The standard calls for ice accretion under normal line voltage and restricts testing to a single flashover per ice layer. Test methods that deviate from this reference approach give some results that are highly correlated and thus useful for insulator selection and comparison after minor adjustment.

In common with clean-fog contamination results, insulator profiles with a ratio of leakage to dry arc distance of 3.3 have the highest flashover stress with light ice accretion of 5 mm. With heavy accretion of 30 mm, all influence of creepage factor is gone as the profiles are all fully bridged with icicles. Leakage distance is thus helpful only for mitigating light and very light icing problems.

Generally, corona rings are not helpful for mitigating icing flashover problems unless they are also screened to inhibit ice formation. Booster sheds perform this function better and at lower cost. Advances in semiconducting coatings and icephobic coatings, based on standard RTV silicone substrate, offer some interesting opportunities for future development of ice-resistant insulators.

ACKNOWLEDGMENT

This lecture summarizes recent progress placed on a strong foundation of knowledge established by more than 200 highly qualified personnel who have collaborated in the NSERC / Hydro-Quebec / UQAC Industrial Chair on Atmospheric Icing of Power Network Equipment (CIGELE) and Canada Research Chair on Atmospheric Icing Engineering of Power Networks (INGIVRE). Development of suitable test methods and standards also relied on the expertise of Insulators WG members in the Overhead Lines subcommittee, Transmission and Distribution Committee of IEEE Power and Energy Society as well as DEIS co-sponsors of IEEE Standards 1783 [33] and P1820 [34].

REFERENCES

- [1] M. Farzaneh, Editor, *Atmospheric Icing of Power Networks*, Berlin:Springer, 2008.
- [2] M. Farzaneh, "Ice accretion on high voltage conductors and insulators and related phenomena", *Phil. Trans. of the Royal Soc.* Vol. 358, No. 1776, pp. 2971-3005, 2000.
- [3] J.S.T. Looms, *Insulators for High Voltage*, London: Peter Perigrinus, 1988.
- [4] CIGRE Working Group 33-04, "The Measurement of Site Pollution Severity and its Application to Insulator Dimensioning for A.C. Systems", *Electra*, No. 64, pp. 101-116, 1979.
- [5] CIGRE Task Force 33.04.03, "Insulators Pollution Monitoring", *Electra*, No. 152, pp. 79-89, 1994.
- [6] CIGRE Task Force 33.04.01, "Polluted Insulators: A Review of Current Knowledge", *CIGRE Technical Brochure*, No. 158, 2000.
- [7] R.S. Gorur, E.A. Cherney, and J.T. Burnham, *Outdoor Insulators*, Phoenix: Ravi S. Gorur Inc., 1999.
- [8] M. Farzaneh and W.A. Chisholm, *Insulators for Icing and Polluted Environments*, New York: IEEE/Wiley, 2009.
- [9] M. Farzaneh and J.-F. Drapeau, "AC Flashover Performance of Insulators Covered with Artificial Ice", *IEEE Transactions on Power Delivery*, Vol. 10, No. 2, April 1995, pp. 1038-1051.
- [10] M. Farzaneh and O.T. Melo, "Properties and Effect of Freezing and Winter Fog on Outline Insulators", *Journal of Cold Regions Science and Technology*, No. 19, Feb. 1990, pp. 33-46.
- [11] M. Kawai, "AC Flashover tests at project UHV on ice-coated insulators", *IEEE Trans. Power App. Syst.*, Vol. PAS-89, No. 8, pp. 1800-1804, Nov. 1970.
- [12] H. M. Schneider, "Artificial ice tests on transmission line insulators – A progress report", IEEE/PES Summer Meeting, San Francisco, USA, No. A75-491-1, pp. 347-353, 1975.
- [13] E. A. Cherney, "Flashover performance of artificially contaminated and iced long-rod transmission line insulators," *IEEE Trans. Power App. Syst.*, Vol. PAS-99, No. 1, pp. 46-52, 1980.
- [14] M. D. Charneski, G. L. Gaibrois, and B. F. Whitney, "Flashover tests of artificially iced insulators," *IEEE Trans. Power App. Syst.*, Vol. PAS-101, No. 8, pp. 2429-2433, Aug. 1982.
- [15] J. F. Drapeau and M. Farzaneh, "Ice accumulation characteristics on Hydro-Quebec H.V insulators," *6th Int. Workshop on the Atmospheric Icing of Structures*, Budapest, Hungary, pp. 225-230, 1993.
- [16] A. Meier and W.M. Niggli, "The influence of snow and ice deposits on supertension transmission line insulator strings with special reference to high altitude operations," *IEEE Conf. Publ. 44*, London, England, pp. 386-395, 1968.
- [17] Z. Vuckovic and Z. Zdravkovic, "Effect of polluted snow and ice accretion on high voltage transmission line insulators," *Proc. 5th Int. Workshop Atmospheric Icing Structures*, Tokyo, Japan, paper B4-3, 1990.
- [18] S. M. Fikke, J. E. Hanssen, and L. Rolfseng, "Long range transported pollutants and conductivity of atmospheric ice on insulators," *IEEE Trans. Power Delivery*, Vol. 8, No. 3, pp. 1311-1321, Jul. 1993.
- [19] D. Wu and R. Hartings, "Correlation between the AC withstand voltage and insulator lengths under icing tests," *Proc. 9th Int. Workshop Atmospheric Icing Structures*, Chester, U.K., p.6, 2000.
- [20] T. Fujimura, K. Naito, Y. Hasegawa, and T. Kawaguchi, "Performance of insulators covered with snow or ice," *IEEE Trans. Power App. Syst.*, Vol. PAS-98, No. 5, pp. 1621-1631, 1979.
- [21] H. Matsuda, H. Komuro, and K. Takasu, "Withstand voltage characteristics of insulator strings covered with snow or ice," *IEEE Trans. Power Delivery*, Vol. 6, No. 3, pp. 1243-1250, 1991.
- [22] L. Shu, C. Sun, J. Zhang, and L. Gu, "AC flashover performance on iced and polluted insulators for high altitude regions", Proc. 7th Int. Symp. High Voltage Eng., Dresden, Germany, pp. 303- 306, 1991.
- [23] CIGRE Task Force 33.04.09, "Influence of Ice and Snow on the Flashover Performance of Outdoor Insulators, Part I: Effects of Ice", *Electra*, No. 187, pp. 91-111, 1999.
- [24] CIGRE Task Force 33.04.09, "Influence of Ice and Snow on the Flashover Performance of Outdoor Insulators, Part II: Effects of Snow", *Electra*, No. 188, pp. 55-69, 2000.
- [25] M. Farzaneh and J. Kiernicki, "Flashover Problems Caused by Ice Build-up on Insulators", *IEEE Electrical Insulation Magazine*, Vol. 11, No. 2, March/April 1995.
- [26] W.A. Chisholm, "North American Operating Experience: Insulator Flashovers in Cold Conditions", CIGRE SC33 Colloquium, Toronto, Canada, 1997.
- [27] S. Yoshida and K. Naito, "Survey of Electrical and Mechanical Failures of Insulators Caused by Ice and/or Snow", CIGRE WG B2.03 Report, *Electra*, No. 222, pp. 22-26, 2005.
- [28] M. Farzaneh (Chair) *et al.*, "Insulator Icing Test Methods and Procedures ». A Position Paper prepared by the IEEE TF on Insulator Icing Test Methods, *IEEE Transactions on Power Delivery*, Vol. 18, No. 4, pp. 1503-1515, October 2003.
- [29] M. Farzaneh (Chair) *et al.*, "Selection of Station Insulators with Respect to Ice or Snow - Part I: Technical Context and Environmental Exposure", A Position paper prepared by IEEE Task Force on Icing

- Performance of Station Insulators, *IEEE Transactions on Power Delivery*, Vol. 20, No. 1, pp. 264-270, Jan. 2005.
- [30] M. Farzaneh (Chair) *et al.*, "Selection of Station Insulators with Respect to Ice or Snow - Part II: Methods of Selection and Options for Mitigation", A Position paper prepared by IEEE Task Force on Icing Performance of Station Insulators, *IEEE Transactions on Power Delivery*, Vol. 20, No. 1, pp. 271-277, Jan. 2005.
- [31] M. Farzaneh (Chair) *et al.*, "Selection of Line Insulators with Respect to Ice and Snow, Part I: Context and Stresses", A position paper prepared by the IEEE Task Force on icing performance of line insulators, *IEEE Transactions on Power Delivery*, Vol. 22, No. 4, pp. 2289-2296, October 2007.
- [32] M. Farzaneh (Chair), *et al.*, "Selection of Line Insulators with Respect to Ice and Snow, Part II: Selection Methods and Mitigation Options", A position paper prepared by the IEEE Task Force on icing performance of line insulators, *IEEE Transactions on Power Delivery*, Vol. 22, No. 4, pp. 2297-2304, October 2007.
- [33] IEEE Standard 1783/2009™, *Guide for Test Methods and Procedures to Evaluate the Electrical Performance of Insulators in Freezing Conditions*, New York: IEEE, Oct. 2009.
- [34] IEEE P1820™/D7, *Draft Guide for Selection of Transmission and Distribution Insulators with Respect to Icing*, December 2012.
- [35] S.M. Fikke, *et al.*, "Guidelines for Field Measurements of Ice Loadings on Overhead Power Line Conductors", CIGRE TF 22.06.01, *CIGRE Technical Brochure*, No. 179, Feb. 2001.
- [36] A. Leblond, *et al.*, "Guidelines for Meteorological Icing Models, Statistical Methods and Topographical Effects", CIGRE TF B2.16, *CIGRE Technical Brochure*, No. 291, April 2006.
- [37] M. Farzaneh, J. Kiernicki, and J.-F. Drapeau, "Ice Accretion on Energized Ice Insulators", *International Journal of Offshore and Polar Engineering*, Vol. 2, No. 3, pp. 228-233, Sept. 1992.
- [38] J.-L. Laforte, C.L. Phan, and J. Druez, "The Effects under dc Electric Field on the Microstructure and Mechanical Properties of Glaze and Rime", Proc. 6th Int. Conf. on Port and Ocean Eng. Under Arctic Conditions, pp. 1057-1066, 1983
- [39] M. Farzaneh and J.-L. Laforte, "Ice Accretion on Conductors Energized by AC or DC: A Laboratory Investigation of Ice Treeing", *International Journal of Offshore and Polar Engineering*, Vol. 4, No. 1, pp. 40-47, March 1994.
- [40] M. Farzaneh & J.-L. Laforte, «The Effect of Voltage Polarity on Ice Accretions on Short String Insulators». *Journal of Offshore Mechanics and Arctic Engineering*, Vol. 113, May 1991, pp. 179-184
- [41] M. Farzaneh & J.-L. Laforte, «Effect of Voltage Polarity on Icicles Grown on Line Insulators». *International Journal of Offshore and Polar Engineering*, Vol. 2, No. 4, pp. 241-246, Dec. 1992.
- [42] P.E. Renner, H. L. Hill and O. Ratz, "Effects of Icing on DC Insulation Strength", *IEEE Transactions on Power Apparatus and Systems*, Vol. PAS - 90 , No.3, pp. 1201-1206, May 1971.
- [43] D. Yu, M. Farzaneh, J. Zhang, L. Shu, W. Sima & C. Sun, «Effects of Space Charge on the Discharge Process in an Icicle/Iced-Plate Electrode System under Positive DC Voltage», *IEEE Transactions on Dielectrics and Electrical Insulation*, Special Issue on Ice-Covered Insulators, Vol. 14, No. 6, pp. 1427-1435, Dec. 2007.
- [44] L. Makkonen, "A Model of Ice Growth", *J. Glaciology*, Vol. 34, p. 116, 1988.
- [45] Y. Teisseire and M. Farzaneh, "On the Mechanism of the Ice Accretion on H.V. Conductors", *Journal of Cold Regions Science and Technology*, No. 18, pp. 1-8, June 1990.
- [46] M. Farzaneh, I. Fofana, I. Ndiaye and K. D. Srivastava, "Experimental investigations of Ice Surface discharge into the Inception and development", *International Journal of Power and Energy Systems*, Vol. 26, No. 1, pp. 34-41, Jan. 2006.
- [47] I. Ndiaye, "Étude de l'apparition et de la propagation de décharges couronnes à la surface de la glace", Mémoire présenté à l'Université du Québec à Chicoutimi comme exigence partielle à l'obtention de la Maîtrise en ingénierie, March 2003.
- [48] M. Farzaneh and I. Fofana, "Study of Insulator Flashovers caused by Atmospheric Ice Accumulation", *Journal of Iranian Association of Electrical and Electronics Engineers*, Iran, Vol. 1, No. 1, pp. 10-23, 2004.
- [49] M. Farzaneh and I. Fofana, "Experimental Study and Analysis of Corona Discharge Parameters on an Ice Surface", *J. Phys. D: Appl. Phys.* Vol. 37, pp. 721-729, 2004.
- [50] S. Brettschneider, Contribution à l'étude de l'apparition et du développement des décharges visibles à la surface de la glace. Ph.D., UQAC, October 2000.
- [51] I. Fofana and M. Farzaneh, "A Simplified Model of Corona Discharge Development on an Ice Surface", in Proc. 2004 Annual Report, IEEE Conference on Electrical Insulation and Dielectric Phenomena, Boulder, Colorado, USA, pp. 667-670, October 17-20th 2004.
- [52] P. V. Hobbs, *Ice Physics*. Clarendon Press, Oxford, 1974.
- [53] J. S. Wetlaufer, "Ice surfaces: macroscopic effects of microscopic structure", *Phil. Trans. R. Soc.*, London, A 357, 3403-3425, 1999.
- [54] V. Sadchenko and G.E. Ewing, "New approach to the study of interfacial melting of ice: infrared spectroscopy", *Can. J. Phys.* Vol. 81: pp. 333-341, 2003.
- [55] S. Farokhi, M. Farzaneh & I. Fofana, "Experimental investigation of the process of arc propagation over an ice surface", *IEEE Transactions on Dielectrics and Electrical insulation*, Vol. 17, No. 2, pp.458-464,Apr. 2010.
- [56] S. Farokhi, M. Farzaneh, and I. Fofana, "Study of ultraviolet emission and visible discharge along an ice surface", *IEEE Conf. Electr. Insul. Dielectr. Phenomena (CEIDP)*, pp. 654-657, 2008
- [57] F.A.M. Rizk, "Mathematical models for pollution flashover" *Electra*, Vol. 78, pp.71-103, 1981
- [58] S. Taheri, M. Farzaneh and I. Fofana, "Equivalent Surface Conductivity of Ice Accumulated on Insulators during Development of AC and DC Flashovers Arcs", *Transactions of Dielectrics and Electrical Insulation* (unpublished)
- [59] M. Farzaneh and J. Zhang, "A Multi-Arc Model for Predicting AC Critical Flashover Voltage of Ice-Covered Insulators", *IEEE Transactions on Dielectrics and Electrical Insulation*, Vol. 14 , No. 6, pp. 1401-1409, Dec. 2007.
- [60] X. Jiang, L. Chen, Z. Zhang, C. Sun and J. Hu, "Equivalence of Influence of Pollution Simulating Methods on DC Flashover Stress of Ice-Covered Insulators", *IEEE Transactions on Power Delivery*, Vol. 25, No. 4, pp. 2113-2120, October 2010.
- [61] X. Jiang, Y. Chao, Z. Zhang, J. Hu and L. Shu, "DC Flashover Performance and Effect of Shed Configuration on Polluted and Ice-covered Composite Insulators at Low Atmospheric Pressure", *IEEE Transactions on Dielectrics and Electrical Insulation*, Vol. 18, No. 1, pp. 97-105, Feb. 2011.
- [62] M. Farzaneh, J. Zhang, and Y. Li, "Effects of low air pressure on ac and dc arc propagation on ice surface," *IEEE Transactions on Dielectrics and Electrical Insulation*, Vol. 12, No. 1, pp. 60-71, Feb. 2005.
- [63] Y. Li, M. Farzaneh, and J. Zhang, "Effects of voltage type and polarity on flashover performances at low atmospheric pressure on an ice surface," *Proc. 8th Int. Offshore and Polar Engineering Conference*, Montreal, Canada, Vol. 11, pp. 543-546, 1998.
- [64] J.P. Nova and G. Ellena, "Arc Field Measurement with a Simple Experimental Apparatus", *Journal of Physics D: Applied Physics*, Vol. 20, No. 4 (April), pp. 462-467, 1987.
- [65] A. Nekahi and M. Farzaneh, "Rotational temperature measurement of an arc formed over an ice surface," *IEEE Transactions on Dielectrics and Electrical Insulation*. Vol. 18, No. 3, pp. 755-759, Jun. 2011.
- [66] A. Nekahi and M. Farzaneh, "Excitation temperature determination of an arc formed over an ice surface using optical emission spectroscopy," *IEEE Transactions on Dielectrics and Electrical Insulation*, Vol. 18, No. 6, pp. 1829-1834, Dec. 2011.
- [67] M. Farzaneh, J. Zhang and X. Chen, "Modeling of the AC Arc Discharge on Ice Surfaces", *IEEE Transactions on Power Delivery*, Vol. 12, pp.325-338, 1997.
- [68] P. Li, J. Fan, W. Ki, Z. Su and J. Zhou, "Flashover Performance of HVDC Iced Insulator Strings", *IEEE Transactions of Dielectrics and Electrical Insulation*, Vol. 14, No. 6, pp. 1334-1338, Dec. 2007.
- [69] R. Wilkins, "Flashover voltage of high-voltage insulators with uniform surface-pollution films," *Proc. IEE*, Vol. 116, No. 3, pp. 457-465, 1969.
- [70] C. Potvin, W.A. Chisholm, P. Prud'homme, M. Farzaneh, D. Lepley, E. Del Bello, "Laboratory testing of EGLA and NGLA under icing and dry conditions for Hydro-Québec TransÉnergie transmission system application", CIGRE International Colloquium on Power Quality and Lightning, Sarajevo, May 13-16 2012.

- [71] M. Farzaneh, I. Fofana, C. Tavakoli, and X. Chen, "Dynamic modeling of DC arc discharge on ice surfaces", *IEEE Transactions on Dielectrics and Electrical Insulation*, Vol. 10, No. 3, pp. 463–474, 2003.
- [72] C. Tavakoli, M. Farzaneh, I. Fofana, and A. Beroual, "Dynamics and modeling of AC arc on surface of ice", *IEEE Transactions on Dielectrics and Electrical Insulation*, Vol. 13, No. 6, pp. 1278–1285, Dec. 2006.
- [73] I. Fofana and A. Béroual, "A Predictive Model of the Positive Discharge in Long Air Gaps under Pure and Oscillating Impulse Shapes", *Journal of Physics. D: Applied Physics.*, Vol. 30, pp. 1653-67, 1997.
- [74] S.Taheri, M. Farzaneh and I. Fofana, "Improved Dynamic Model of DC Arc Discharge on Ice-covered Post Insulator Surfaces", *IEEE Transactions on Dielectrics and Electrical Insulation* (in press)
- [75] C.S. Engelbrecht, I. Gutman and R. Hartings, "A Practical Implementation of Statistical Principles to Select Insulators with respect to Polluted Conditions on Overhead ac Lines," *Proceedings of IEEE PowerTech 2005*, St. Petersburg, Russia, paper 129. June 27-30, 2005.
- [76] M. Farzaneh. and W.A. Chisholm, "Effects of Ice and Snow on the Electrical Performance of Power Network Insulators", Chapter 7, *Atmospheric Icing of Power Networks*, Berlin:Springer, pp. 269-325, 2008.
- [77] IEEE Standard 4/2013TM, *IEEE Standard for High-Voltage Testing Techniques*, New York: IEEE, May 2013.
- [78] X. Jiang, M. Bi, J. Hu, Z. Zhang and Y. Xia, "Influence of Test Methods on DC Flashover Performance of Ice-covered Composite Insulators and Statistical Analysis", *IEEE Transactions on Dielectrics and Electrical Insulation* , Vol. 19 , No. 6, pp. 2019-2028, Dec. 2012.
- [79] A. C. Baker, M. Farzaneh, R. S. Gorur, S. M. Gubanski, R. J. Hill, G. G. Karady, and H. M. Schneider, "Insulator Selection for AC Overhead Lines with Respect to Contamination", *IEEE Transactions on Power Delivery*, Vol. 24, No. 3, pp. 1633-1641, July 2009.
- [80] Q. Hu, L. Shu, X. Jiang, C. Sun, Z. Zhang and J. Hu, "Effects of Shed Configuration on AC Flashover Performance of Ice-covered Composite Long-rod Insulators", *IEEE Transactions of Dielectrics and Electrical Insulation*, Vol. 19, No. 1, pp. 200-207, Feb. 2012.
- [81] H. Akkal, C. Volat and M. Farzaneh, "Improving Electrical Performance of EHV Post Station Insulators under Severe Icing Conditions Using Modified Grading Rings", *IEEE Transactions on Dielectrics and Electrical Insulation* , Vol. 20 , No. 1, pp. 221 – 228, Feb. 2013.
- [82] Z. Xu, Z. Jia, Z. Li, X. Wei, Z. Guan and M. MacAlpine, "Anti-icing Performance of RTV Coatings on Porcelain Insulators by Controlling the Leakage Current", *IEEE Transactions of Dielectrics and Electrical Insulation*, Vol. 18, No. 3, pp. 760-766, June 2011.
- [83] G.Momen and M. Farzaneh, "Survey of micro/nano filler use to improve silicone rubber for outdoor insulators", *Reviews on Advanced Materials Science*, Vol. 27, No.1, pp.1-13, 2011.
- [84] CIGRE WG D1.45, "Testing of insulator performance under heavy rain" (unpublished)
- [85] T. Xu, H-M. Wang, L-L. Wang, Z-M. Xu, T. Yao and L. Cai, "Flashover Performance of 500 kV Ice-covered Porcelain Post Insulators with Composite Assistant Shed", *High Voltage Engineering*, Vol. 38, No. 1, pp. 167-172, Jan. 2012.



Masoud Farzaneh is Director-founder of the International Research Center CENGIVRE, Chairholder of the NSERC/Hydro-Quebec/UQAC Industrial Research Chair CIGELE and Chairholder of the Canada Research Chair INGIVRE related to power transmission engineering in cold climate regions. His field of research encompasses high voltage and power engineering including the impact of cold climate on overhead transmission lines. He authored or co-authored more than 500 technical papers, and 17 books or book chapters. Prof. Farzaneh has so far trained more than 100 postgraduate students and postdoctoral fellows. Actively involved with CIGRÉ and IEEE, he is Convenor of CIGRE WG B2.44 on coatings for protection of overhead lines during winter conditions, and member of the Executive Committee of CIGRE Canada. He is currently President of IEEE DEIS, and member of the Editorial Board of IEEE Transactions on Dielectrics and Electrical

Insulation. He is Fellow of IEEE, Fellow of The Institution of Engineering and Technology (IET) and Fellow of the Engineering Institute of Canada (EIC). His contributions and achievements in research and teaching have been recognized by the attribution of a number of prestigious prizes and awards at national and international levels.